Optical Phase Lock Loop For Atom Inteferometry

A Thesis

submitted to

Indian Institute of Science Education and Research Pune

in partial fulfillment of the requirements for the

BS-MS Dual Degree Programme

by

Anurag Nitinrao Bhadane

Indian Institute of Science Education and Research Pune

Dr. Homi Bhabha Road,

Pashan, Pune 411008, INDIA.

April, 2022

Supervisor: Dr. Umakant D. Rapol

© Anurag Nitinrao Bhadane   2022

Certificate

This is to certify that this dissertation entitled Optical Phase Lock Loop For Atom Inteferometry towards the partial fulfilment of the BS-MS dual degree programme at the Indian Institute of Science Education and Research, Pune represents study/work carried out by Anurag Nitinrao Bhadane at Indian Institute of Science Education and Research under the supervision of Dr. Umakant D. Rapol, Associated Professor, Department of Physics, during the academic year 2021-2022.
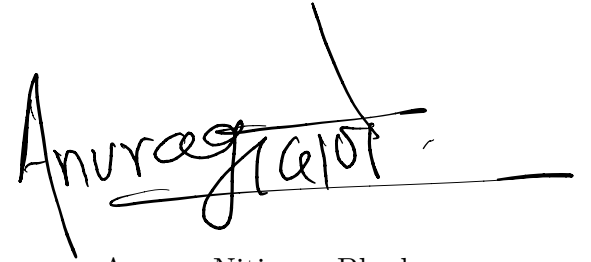
Dr. Umakant D. Rapol

Committee:

Dr. Umakant D. Rapol

Dr. Sunil Nair

This thesis is dedicated to Father, Mother, Grandmother, Grandfather and Sister

Declaration

I hereby declare that the matter embodied in the report entitled Optical Phase Lock Loop For Atom Inteferometry   are the results of the work carried out by me at the Department of Physics, Indian Institute of Science Education and Research, Pune, under the supervision of Dr. Umakant D. Rapol and the same has not been submitted elsewhere for any other degree.

Anurag Nitinrao Bhadane

Acknowledgments

I would like to thank Dr. Umakant Rapol for giving me a wonderful opportunity to work in his lab as a master's student. Umakant sir not only taught me to work independently but to work hard. As well as would like to give thanks to my seniors including Korak Biswas, Pranab Datta, Kushal Patel, and Shiv Sagar Maurya for their invaluable help.

I would like to thank the IISER Pune for its BS-MS program.

x

Abstract

Atom based gravimeter is one of the prominent candidates to measure the local acceleration due to gravity. There are two types of atom bases gravimeter, Cold atom-based gravimeter, and the Bose-Einstein-Condensate(BEC) gravimeter. Gravimeter works on the principle of the diffraction of atomic cloud by optical grating. The noise in gravimeter depends on many factors out of which one is the phase noise in optical gratings caused by acoustic vibrations. The lower the noise better the precision.

In this thesis we implement the Optical Phase Lock Loop(OPLL) to reduce the acoustic phase noise and the instrumentation for the optical phase lock loop is shown. The setup's primary goal is to lock the phase of optical grating.

Contents

List of Figures

1

List of Tables

Chapter 1

Introduction

The ultra-cold atom-based gravimeter is one of the most precise gravimeters around the world. The gravimeter is based on the Mach-Zehnder interferometer. The ultra-cold atoms based Mach-Zehnder interferometer(MZAI) is similar to the light-based interferometer, except for the role of the light and matter is reversed. In MZAI one uses three pulses of moving optical lattice to coherently split, reflect and merge the atomic wavepackets. Here the moving optical lattices act as mirror and beam-splitter and the atom mimics the role of light. The sensitivity of the atom-based interferometer is 10^{11} times higher than a light interferometer. The accurate gravity measurement has a wide variety of usage in civilian applications. The prominent civilian applications are in hydrology, oil and mineral exploration, gravity mapping, etc. There are two prominent ways of atom interferometry(AI) around the world: One is based on the Raman transition and the other is based on the Bragg diffraction.

In Raman diffracted AI, the atoms fall under gravity where one uses three pulses of Raman beam which targets two hyperfine ground states $|5^2S_{1/2}, F = 1\rangle$ & $|5^2S_{1/2}, F = 2\rangle$ of ^{87}Rb atom [1]. Figure 1.1 describes a three-level system where $|1\rangle$ and $|2\rangle$ are two hyperfine ground states of ^{87}Rb and $|e\rangle$ describes the excited level. Here one uses counter-propagating beams of light which are phase-locked to each other. (The two counter-propagating lasers can be generated using different mechanisms such as optical phase locking(OPLL) [2], acousto-optic modulators (AOM), and electro-optic modulators (EOM) [3]). In case of ^{87}Rb the two hyperfine states have a frequency difference of 6.8346 GHz. One method to do so is two have two laser sources named master laser and slave laser. The master laser is frequency
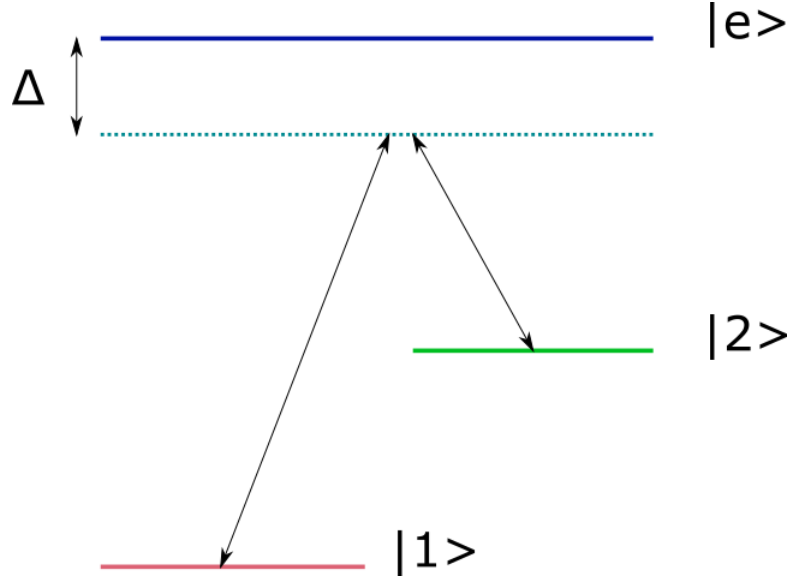
Figure 1.1: Raman Transition of two level system with $|1\rangle$ as ground state and $|2\rangle$ as excited state coupled by two photon process.

locked through the frequency-modulation (FM) spectroscopy technology. Locking of the slave laser with respect to the master laser can be done in various ways. One of the ways to lock to the laser is by generating a beat signal of 6.8 GHz standard by EOM. Electro-Optic-Modulator(EOM) can also be used for generation of slave laser. The EOM is driven by the 6.8 GHz signal and the sideband is created with it.

The atoms are subjected to three pulses made up of sequence $\pi/2$-π-$\pi/2$ pulse [4]. Three corresponding pulses are Rabi pulses which alter the population of the states depending upon the time of interaction. The pulses such as $\pi/2$ split the atoms equally in the ground as well as in an excited state, which act as the beamsplitter whereas the π pulse inverts the whole population, act as a mirror.

Bragg diffraction is an analogous scheme for atom interferometer[5]. For BEC Bragg diffraction works on the principle of the Bogoliubov excitation [6]. During Bragg transition, the atoms are transferred to nth order momentum states using 2n-photon transition by allowing one photon to be absorbed and perform a stimulated emission using another photon. The transition of the two-photon system gives the momentum kick.[7]

The difference between two counter-propagating frequencies is decided by the following equation-1.1 and 1.2.

The Rubidium Bose-Einstein-Condensate is also subjected to the three pulse sequence made
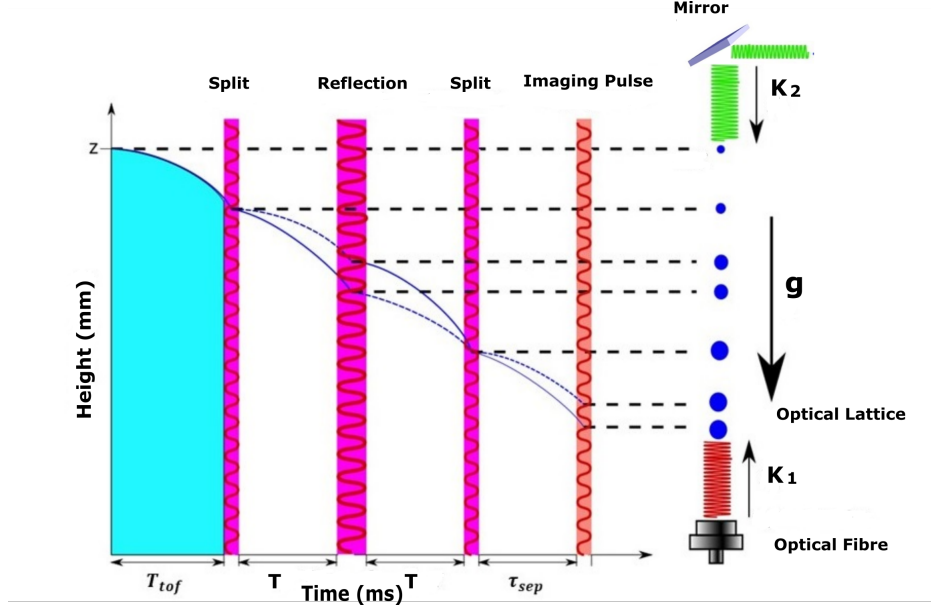
Figure 1.2: Mach-Zehnder Inteferometer. The BEC is released from the top, after T_{tof} split($\pi/2$) pulse is applied. The pulse coherently separates wavepackets in two momentum states. The reflection pulse(π) pulse inverts the momentum of wavepackets. The time T between two pulses is interferogram time. At the end imaging pulse detects the phase of AI.

up of $\pi/2$-π-$\pi/2$ pulses [8].

$$\frac{(nP_r)^2}{2M} = n\hbar\delta_n \tag{1.1}$$

where,

$$P_r = 2\hbar k sin(\frac{\theta}{2}) \tag{1.2}$$

The P_r is the recoil momentum, M is the mass of the atom used for the BEC, δ_n is the detuning required for the optical lattices. For ^{87}Rb and angle of 180^0, the value of δ_n is 15kHz.

The Mach-Zehnder Interferometer's mirror and beam-splitter are given by duration of optical lattices. The following diagram explains the ultra-cold atom based gravimeter.

The BEC is released for some amount of time τ called as time of flight, to remove the mean-field energy[8]. The split pulse or $\pi/2$ pulse separates the BEC into two momentum states. The "Reflect" or π pulse reverses the population of the momentum state followed by

7

the $\pi/2$ pulse. The last pulse is the detection pulse which detects the spatial separation of the two wave-packets.

At each experiment, the vibrations caused by the mirrors changes the phase of the laser beam. The following Figure 1.2 tells about the phase noises in the system that are caused by the acoustic noises and vibrations.

So initial phase that gets imparted on the two $\pi/2$ pulses is different for each experiment. The goal of this thesis is to create the locking system such that at each time the experiment's initial phase is locked to the particular phase value.

Chapter 2

Atom Interferometry with Ultra-cold atoms

2.1 Light matter interaction

The interaction of the atoms with light is at the heart of the atom interferometry. The Atom interferometry works on the principle of diffraction by optical grating. Before that simple Rabi oscillation review is necessary.

2.1.1 Two level atoms in a laser/light field

The Schrodinger's equation states the dynamics of the quantum particles and is given by,

$$-i\hbar\frac{\partial \psi}{\partial t} = H\psi \tag{2.1}$$

Energy levels of the electron sees the perturbation caused by light as V.

$$H = H_0 + V(r) \tag{2.2}$$

Let $c_1(t)$ and $c_2(t)$ be the probabilities of the electron to be in energy levels of $|g\rangle$ and $|e\rangle$ respectively. The equation of the dynamics of the probabilities is given as [9],

$$\dot{c}_1(t) = -\frac{i}{\hbar} \left(c_1(t)V_{11} + c_2(t)V_{12}exp(-iw_0t) \right) \tag{2.3}$$

$$\dot{c}_2(t) = \frac{i}{\hbar} \left(c_1(t)V_{21}exp(iw_0t) + c2(t)V_{22} \right) \tag{2.4}$$

where,

$$V_{ij} = \langle \psi_i|V|\psi_j \rangle$$

The use of semi-classical approach simplifies the problem. Light-atom interaction term V can be given as

$$V = e\vec{r}.\vec{\varepsilon}(t) \tag{2.5}$$

by substituting $\vec{\varepsilon} = \varepsilon_0 cos(\omega t)$ and simplifying we get the following equations.

$$V_{ij} = -\frac{\varepsilon_0}{2} \left(exp(-i\omega_0t) + exp(i\omega_0t) \right) \mu_{ij} \tag{2.6}$$

$$\dot{c}_1(t) = i\frac{\varepsilon_0\mu_{12}}{2\hbar} \left(exp(i(\omega - \omega_0)t) + exp(-i(\omega + \omega_0)t) \right) \tag{2.7}$$

$$\dot{c}_2(t) = i\frac{\varepsilon_0\mu_{12}}{2\hbar} \left(exp(-i(\omega - \omega_0)t) + exp(i(\omega + \omega_0)t) \right) \tag{2.8}$$

The term Rabi frequency is given by,

$$\Omega_r = \frac{\varepsilon_0|\mu_{12}|}{\hbar} \tag{2.9}$$

By using rotating field approximation and strong electric field we get [1]

$$|c_1(t)|^2 = cos^2\left(\frac{\Omega_rt}{2}\right) \tag{2.10}$$

$$|c_2(t)|^2 = sin^2\left(\frac{\Omega_rt}{2}\right) \tag{2.11}$$

and can also be written as the

$$|c_1(t)|^2 = \frac{1}{2}(1 - cos(\Omega_r t)) \tag{2.12}$$

$$|c_2(t)|^2 = \frac{1}{2}(1 + cos(\Omega_r t)) \tag{2.13}$$

Interaction time t decides the population of excited state and ground state, so after $\tau = \frac{\pi}{\Omega_r}$ population of electronic levels completely inverts and is called as π pulse.

For $\pi/2 = \Omega_r t$ pulse the population gets divided into to equal populations. The analogy between simple Rabi oscillation and the Bragg diffraction is very essential. The Bragg diffraction also works with a similar principle but on virtual levels.

2.1.2 Matrix Formulation

The atom laser interaction is the core of the atom interferometer. The interaction of laser beams imparts the population change in the ground and excited state. Let $c_g(t)$ and $c_e(t)$ be the ground state and excited population. Time evolution of two states can be given by the

$$\begin{pmatrix} c_g(t) \\ c_e(t) \end{pmatrix} = M \begin{pmatrix} c_g(0) \\ c_e(0) \end{pmatrix}$$

M is the interaction matrix between laser light and atom and is given by ,

$$M = \begin{bmatrix} \left(cos\left(\left(\frac{\Omega_f t}{2}\right)\right) - i\frac{\delta}{\Omega_f}sin\left(\frac{\Omega_f t}{2}\right)\right)e^{\left(\frac{i\delta t}{2}\right)} & -i\frac{\Omega}{\Omega_f}e^{-i\phi}e^{\frac{i\delta t}{2}}sin\left(\frac{\Omega_f t}{2}\right) \\ -i\frac{\Omega}{\Omega_f}e^{-i\phi}e^{\frac{i\delta t}{2}}sin\left(\frac{\Omega_f t}{2}\right) & \left(cos\left(\left(\frac{\Omega_f t}{2}\right)\right) + i\frac{\delta}{\Omega_f}sin\left(\frac{\Omega_f t}{2}\right)\right)e^{\left(\frac{-i\delta t}{2}\right)} \end{bmatrix}$$

whereas the δ is detuning of the laser beam, Ω_f is Rabi oscillation and t is the interaction time.

The interaction time of the laser and two-level atoms decides the population dynamics. For particular pulse duration and power, we can split the two states in equal population, invert the population from ground state to excited state, and vice versa. The pulse duration in which the division of equal population happens is called the $\pi/2$ pulse.

$$M = \frac{1}{\sqrt{2}}\begin{bmatrix} 1 & -ie^{-i\phi} \\ -ie^{-i\phi} & 1 \end{bmatrix}$$

11

.

Similarly if the inversion of population happens pulse is called as the π pulse. The matrix form after all substitution can be given as,

$$M = \begin{bmatrix} 0 & -ie^{-i\phi} \\ -ie^{-i\phi} & 0 \end{bmatrix}$$

2.1.3   Three level system / atom interferometry

Three-level system is a generalization of two-level systems. The three level system is driven by two photon transition. The three-level system requires two lasers. The slave laser is locked to master level. Master and slave laser are detuned by the 6.8 GHz hyperfine splitting between F=1 and F=2. The master laser is highly detuned from the resonance transition to reduce the spontaneous emission and has momentum of $\hbar k_1$ and slave with $\hbar k_2$. When atom gets excited from state $|1\rangle$ to $|2\rangle$ it gains the energy and some momentum. for $k_1 = -k_2$ the following equations are given,
The two level system give rise to effective Rabi oscillation with Ω_{eff} frequency.

$$\text{Energy} = \hbar \left(\omega_e - \omega_g \right) \tag{2.14}$$

$$\text{Momentum} = \hbar \left(k_1 - k_2 \right) = 2\hbar k_1 \tag{2.15}$$

$$\phi_{eff} = \phi_1 - \phi_2 \tag{2.16}$$

The pulse sequence of atom interferometer is $\pi/2$ - π - $\pi/2$ and explained in the Figure 2.1 . As we know that $\pi/2$ pulse coherently splits the atomic cloud in two states, the excited state atoms comes with momentum change as there are half of the atoms at the excited states, the half of the cloud gains momentum kick. While happening all this the atomic cloud descent in gravity and gains some separation. The next π pulse inverts the two population levels. The ground state atoms make transition to the excited state and the excited state atoms to ground state. The third $\pi/2$ pulse makes the interference in the two atomic clouds. The chirping frequency is needed to balance the Doppler shift caused by the gravity. At particular chirping frequency the phase of the interferometer becomes zero.
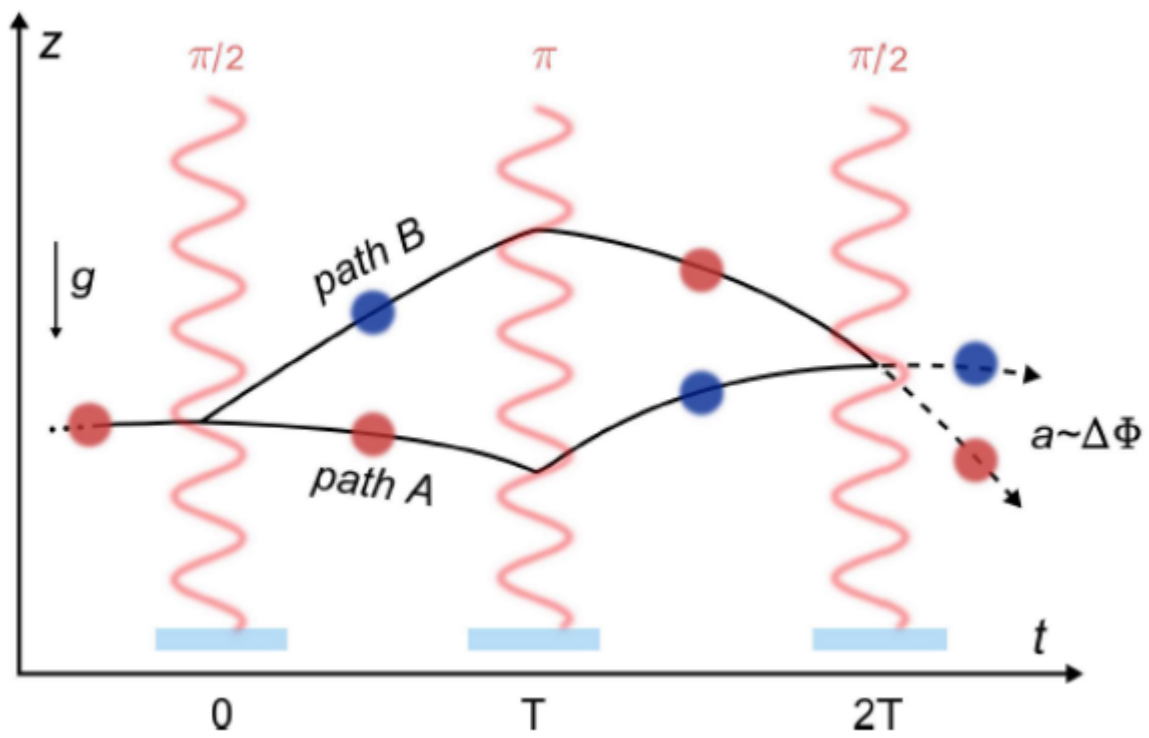
Figure 2.1: Atom Interferometer. The path followed by A and B is not horizontal but vertical.

2.2 Bragg Diffraction

Similar to the Raman Interferometer the Bragg Interferometer can also be used for the gravimeter[10]. The main difference from the Raman-based interferometer is the use of Bose-Einstein-Condensate(BEC) instead of cold-atoms. The Bragg gravimeter works on the principle of the Bragg diffraction[11]. One beam causes the excitation of the condensate and other stimulated emission to other states. The process is similar to two photon transition except the two levels are at ground and happens between $|g, 0\rangle$ and $|g, 2\hbar k\rangle$. In case of Raman-based diffraction the transition happens between a ground state and excited state. After optical lattice pulse momentum is gained by the one wavepacket. For Bragg diffraction, the light is highly detuned from the transition to lower the probability of the spontaneous emission. The $\pi/2$ pulse and π pulses values calculated varying the detuning and the intensity of the laser beam. Compared to the Raman pulses the Bragg pulses are much longer and are usually of range of μs.

2.2.1 Chirping frequency and acceleration due to gravity

The falling BEC is accelerating in gravity and sees the Doppler shift in an incoming laser beam. The laser with varying frequency balances the effect of the gravity. The necessary modulation required for the optical lattice beam is called as the chirping frequency. The chirping frequency for a particular wavelength is calculated by the following formula.

$$\alpha = \frac{\vec{k}.\vec{g}}{\pi} \tag{2.17}$$

where $\vec{k} = \frac{2\pi}{\lambda}$, and the value of α for Rubidium atom for 780 nm optical grating is 25.1 MHz/s.

2.2.2 Atom Interferometery

Similar to the Raman-bases interferometer, the Bragg interferometer works. The pulse sequence remains same as π-π-$\pi/2$. The basic interferometric scheme is given below, The $\pi/2$ pulse coherently splits the atomic cloud into half-half atomic wave packets, one packet with no momentum gain and one with $2\hbar k$ momentum. After time period of T, π pulse interacts with both atomic wave-packets, which inverts the population of momentum levels. The in-

version comes with a change of momentum. The atomic wave-packet with no momentum, gains $2\hbar\vec{k}$ momentum and vice versa. Again at the last a π pulse is subjected to the atomic wave-packet which interferes two wavepackets. The spatial separation of the wave-packets happens with time because of momentum transfer from photons to atoms. The total phase gained by the interferometer at the end is given by [4]

$$\phi = \omega_{eff}t - k_{eff}z + \phi_{eff} \tag{2.18}$$

$$z = \frac{1}{2}gT^2 \tag{2.19}$$

$$\phi = \omega_{eff}t - k_1 gT^2 + \phi_{eff} \tag{2.20}$$

The total phase gathered at the end of the interferometer is given by, for Bragg AI ϕ_{eff} is effectively zero as there are no master and slave laser and ω_{eff} remains constant.

The combination of $\pi/2 - \pi - \pi/2$ pulses creates the Mach-Zehnder Interferometer. The total phase gathered by the population of the two momentum states is given by,

$$\phi = \vec{k}.\vec{g}T^2 \tag{2.21}$$

If we are also applying the chirping frequency, the total phase gathered is given by the,

$$\phi = \vec{k}.\vec{g}T^2 - 2\pi\alpha T^2 \tag{2.22}$$

The value of the g is calculated at $\phi = 0$. There are many ϕ values with a given condition. The single value of g is fixed by considering at least three atom interferometry data with variable interferogram time.

2.2.3   Noise in acceleration due to gravity

The mirrors, beamsplitters present in the setup are always at vibrations because of the thermal temperature, acoustic noises. This imparts the error in the phases of the Bragg pulses. The Bragg pulses at different experiment times might not have the same phase when they interact with BEC. This causes errors in the final population. The aim of this thesis is to reduce the noises that are coupled with vibrations and acoustic sources. The following graph explains the noises at different frequencies. The data was recorded on a photodiode and recorded on the oscilloscope.
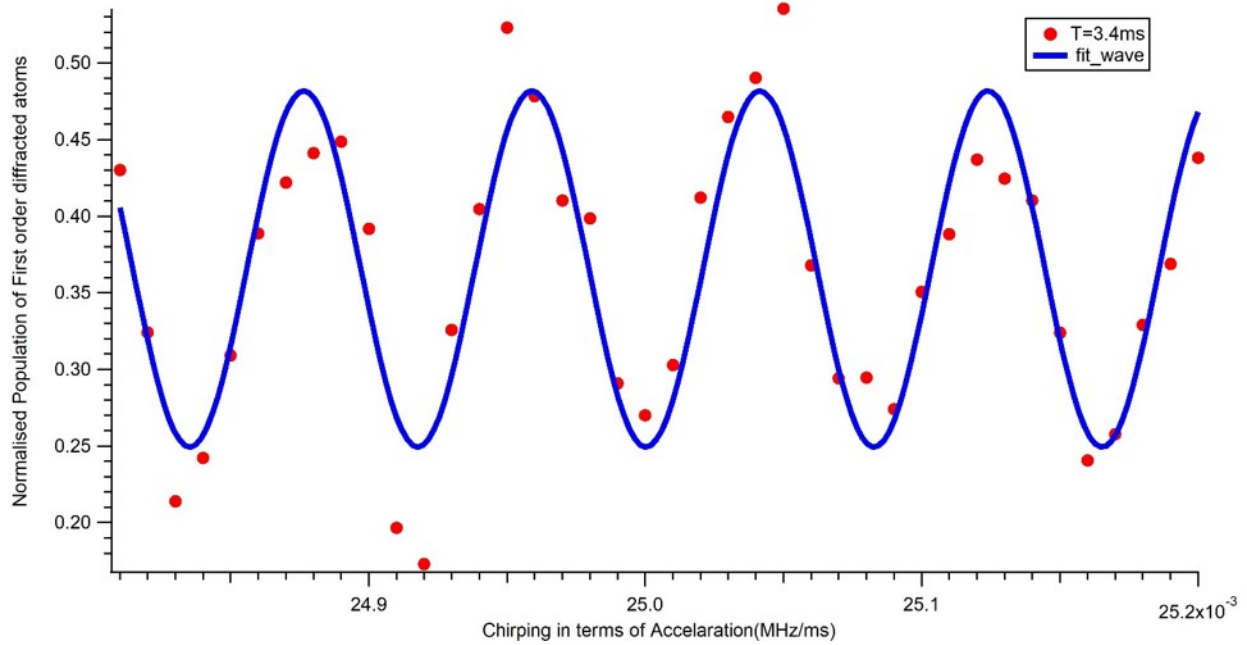
Figure 2.2: Phase vs chirping frequency. As shown in the graph the phase ϕ has multiple minima's. The accurate value of chirping frequency needed to balance the acceleration due to gravity is calculated from multiple different interferogram time.The Interferometer time is T = 3.4ms for current AI is 3.4ms.
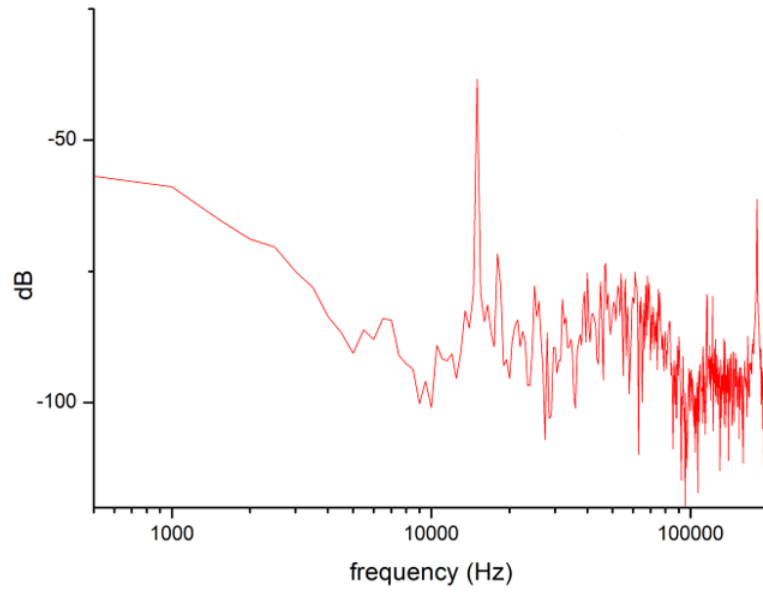
Phase noises of optical lattice beams. Phase noise caused by acoustic noise at lower frequencies. Beat frequency is at 15 kHz

Chapter 3

Experimental setup

In this chapter, we will see the experimental setup for the optical phase lock loop and some experimental results.

3.1   Optical Phase Lock Loop

The optical phase lock loop is a method to lock the phase of the laser beam with respect to a particular value and has been implemented for the various setups [12]. The main goal of this project is to lock the Bragg beams to the initial phase. The setup is consists of electronic and optical circuits. The optical circuit will consist of Mach-Zehnder Interferometer. The two counter-propagating beams are generated by AOM and the response of the beat signal is recorded on the photodiode. Other than the given OPLL scheme there is another scheme as well. The other scheme uses an Electro-Optic-Modulator(EOM) instead of an Analog Phase Shifter (APS). The EOM imparts phase directly to the laser beam. The EOM requires an EOM driver. Here we are proceeding with the analog phase shifter scheme. If we proceed with EOM, the output of PID should be fed into the EOM driver instead of the analog phase shifter.
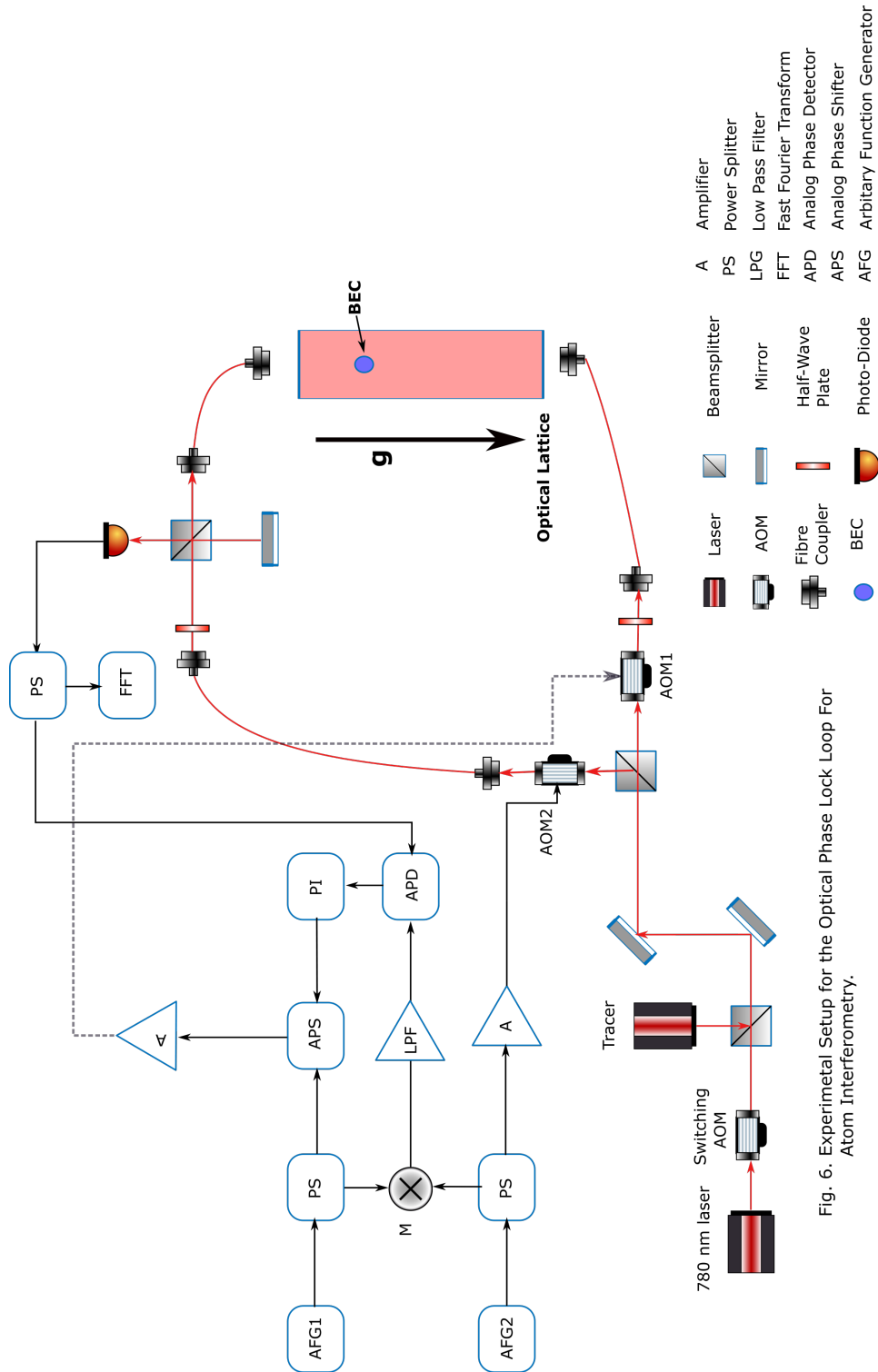
Fig. 6. Experimetal Setup for the Optical Phase Lock Loop For Atom Interferometry.

The AFG1 and AFG2 are two arbitrary waveform generators locked to each other by a phase lock loop. The external clock is used made of rubidium standard. Out of two AFG's

one generates a signal of 80 MHz and another one generates a signal of 80.015 MHz. The power splitter taps some power out of the output signal of the AFG's. The mixer mixes the output of AFG's and creates multiple frequency components, one with $f_1 + f_2$ and another with $f_1 - f_2$. After applying the low pass filter, select only $f_1 - f_2$ component. The lower frequency $f_1 - f_2$ component becomes the reference of the analog phase detector. The whole system is locked to this lower frequency component of the mixer. The analog phase detector compares the phase difference between a reference signal and a photodiode signal.

Now we will move towards the optical circuit as the other test signal is coming photodiode. For a Bragg diffraction, we are using the 780 nm light detuned from the transitions. The Bragg pulses are only on for some microseconds, so we need a "reference" laser beam. The reference beam is generated by the 790 nm laser beam which is independently locked. The reference "tracer" beam traverses the same path as the Bragg beam so the phase noises caused by the vibrations of the mirror impart the same fluctuations as wavelength are nearly the same. The tracer beams' power is very small and the effect on the Rb BEC is small. The Bragg beams are made on-off by control over AOM. The 780 nm laser beam is further divided into two beams to generated 80 MHz and 80.015 MHz. These two beams are coupled to Rb BEC and an optical lattice is formed. The beat signal is recorded on the photodiode. The photodiode signal is fed to the analog phase detector.

Now again after getting two signals, the analog phase shifter will be followed by PI. The PI will be locked to the particular phase and depending on the phase, PI will change the phase of the analog phase shifter. The analog phase shifter's output will pass the thought amplifier then to AOM.

3.2   Laser System

As a reference system, we need a tracer beam, which will follow the same path as the standing traveling waves. The tracer beam is independently locked and is of the wavelength of 790 nm[13]. Laser is made of the DL100 a toptica based laser controller and laser mounting system. Here in this section, we will see the construction of the laser diode system.

3.2.1   Laser Diode

Laser diode is a versatile source of generation of the coherent beam of light. These laser diodes are handy and easily transportable. Diode laser comes in wide ranges of wavelength starting from 200 nm to 4000 nm. Unfortunately, diode lasers do not come with fixed wavelengths, diode lasers can have a big range of wavelength spectrum. The line-width of the diode laser can be reduced with an external cavity.

3.2.2   Mode selection

As laser diode has various output frequencies, the single-mode application is necessary for experiments of gravimeters. The single-mode requires some sort of "feedback" or "reference", the mode of references are given below,

- **Injection Locking** An external laser source supplies reference for the diode laser. The seed laser of the single longitudinal mode is coupled into the diode laser.

- **External Grating** The output beam of the laser beam is diffracted by the desired grating. Gratings' first order is fed to the laser diode and reflected order is the output of the overall diode laser. An external grating's diffracted order and laser diodes internal cavity form the cavity which selects particular modes over others.

Here we are going to make a laser diode laser with external grating. The mode selection of the laser diode output is decided by the grating which is placed outside the laser diode. The grating diffracts the output of the laser diode into various angles depending on the wavelength.

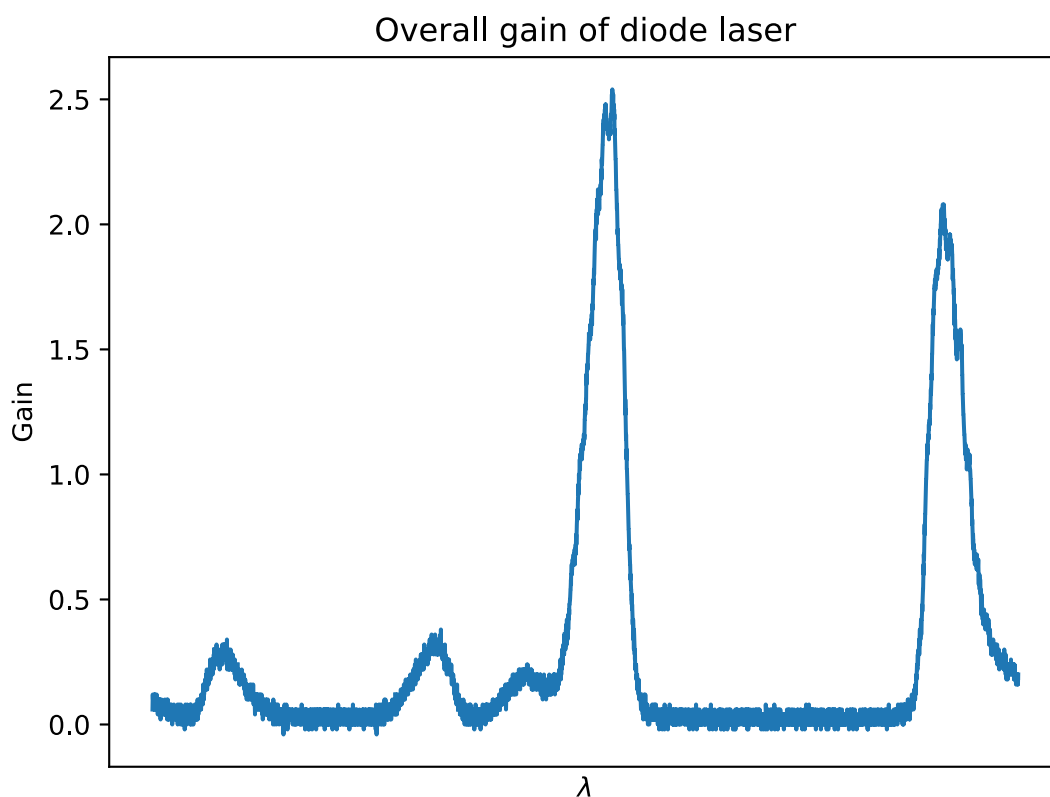$$n\lambda = d sin(\theta) \tag{3.1}$$

Figure 3.1: Mode selection. The overall gain mode of 780 nm laser. The mode's amplitude does not remain constant throughout the spectrum.

The θ is diffracted angle for wavelength λ, whereas d is the distance between two gratings. The diffracted beam is direct towards the laser diode. The grating gives gain for selected diffracted wavelengths. The gain of the medium, internal modes of the laser diode, external modes of the laser diode selects overall mode selection. The modes can be changed with help of the current of the diode, the temperature of the diode, and grating feedback.

The graph that is given above represents the gain of 780nm laser beam. Note that for each and every wavelength gain is not uniform.

3.2.3 Feedback and Lasing

The feedback is necessary for the stability of output laser frequency. If not the laser diode output will be in multi-mode. There are some advantages and disadvantages of using the multi modes and single-mode lasers. The multimode lasers are easy to construct and have much more power than the single-mode lasers but the multimode lasers have power spread throughout some frequency range. Tracer beam requires the low power not to affect the Rb Bose-Einstein condensate as well single mode application for the working of OPLL. The feedback is provided by the grating's diffracted order. The lasing of the diode is the minimum excitation level after which the output of the diode laser is dominated by the stimulated emission. Better is the feedback lower is the lasing current.

3.3 Analog Phase Detector

The AD630 is balanced modulator/demodulator [14] can be used for the phase extraction. The modulator is a device that modulates the "message" signal with a carrier signal. The same principle is used in radio communication and a demodulator is a device that extracts a "message" signal from the modulated signal. We can get information on the phase from the Modulator. The math of the problem is given below.

The AD630 works on the principle of Amplitude modulation. Let carrier signal is given by the c and photodiode signal is given by the m(t).

$$c(t) = A\sin(2\pi f_c t) \tag{3.2}$$

similarly, message signal can be represented as

$$m(t) = M\sin(2\pi f_m t + \phi) \tag{3.3}$$

The amplitude modulation signal can be written as

$$y(t) = c(t) \left[1 + \frac{m(t)}{A} \right] \tag{3.4}$$

After putting the values of the carrier and modulating the signal we get,

$$y(t) = A\sin(2\pi f_c t) \left[1 + m\cos(2\pi f_m t + \phi) \right] \tag{3.5}$$

After simplifying this equation we get

$$y(t) = A\sin(2\pi f_c t) + \frac{1}{2} Am \left[\sin(2\pi \left(f_c + f_m \right) t + \phi) + \sin(2\pi \left(f_c - f_m \right) t - \phi) \right] \tag{3.6}$$

By putting $f_c = f_m$, we can simplify the equation as below,

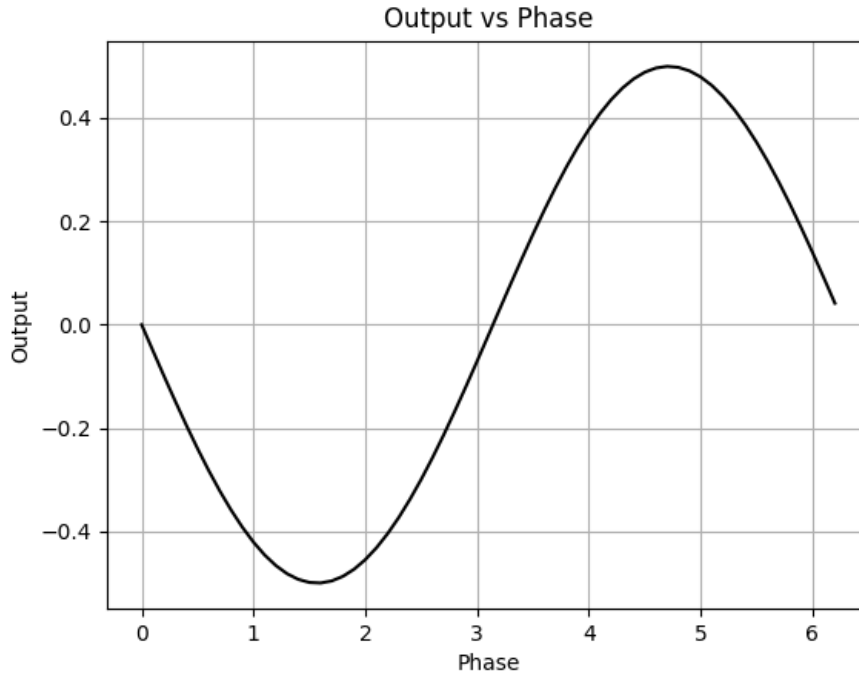$$y(t) = A\sin(2\pi f_c t) + \frac{1}{2} Am \left[\sin(4\pi f_c t + \phi) - \sin(\phi) \right] \tag{3.7}$$

Figure 3.2: Output of the amplitude modulation. The higher frequency components are cancelled by low pass filter.

$$y(t) = Asin(2\pi f_c t) + \frac{1}{2}Amsin(4\pi f_c t + \phi) - \frac{1}{2}Amsin(\phi) \tag{3.8}$$

By applying the low pass filter we can get the information of the phase given in Figure 3.2.

The output of the analog phase detector has a periodic form. The phase information is hidden inside the DC/Offset level of the signal. The beat signal generated by the interference pattern is of 15 kHz. A modulator made up of AD630 (Figure 3.3) will generate a 30 kHz signal. There are two ways from which we can extract information out of the waves and given below.

The photodiode signal is fed into the modulation input of AD630 and the reference signal is fed into the carrier input. As we know that AD630 works on the principle of modulation/demodulation. The current circuit works as a modulates the incoming signal.
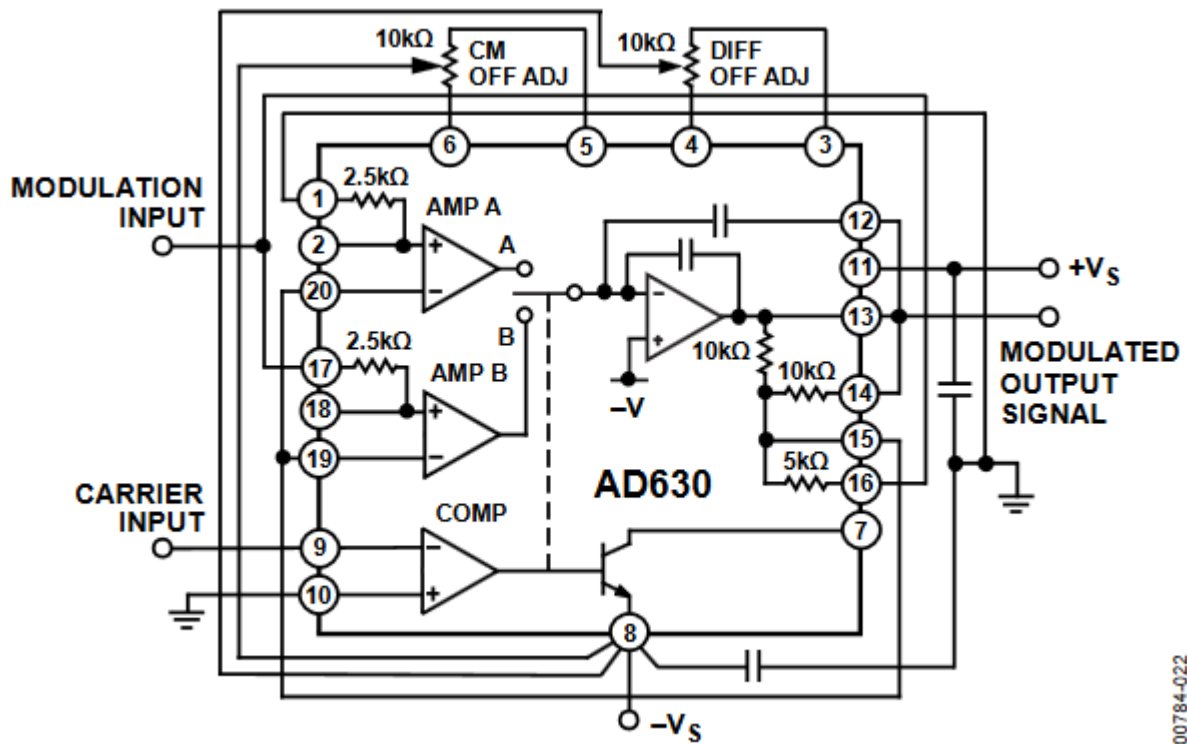
Figure 3.3: AD630 as balanced modulator. The reference is faded into carrier input and photodiode signal into modulation input.

3.4 Phase extraction

3.4.1 Low pass filter

A low pass filter is one of the simplest methods to be used for the extraction of phase. The op-amp-based active low pass filter not only gives the freedom of cutoff frequency but pole order also. The low pass filter is defined by its cutoff frequency. The simple design of the low pass filter is given in Figure 3.4. The resistor and capacitor form a simple low pass filter. The working of the low pass filter depends on the variable impedance for variable frequency. The impedance of the capacitor depends on the frequency of the voltage signal. The impedance of the capacitor is given by the $1/\omega C$. The lower the frequency is more is the impedance. For lower frequency, the input signal does not prefer to pass through the capacitor but as the frequency of the voltage signal increases the impedance of the capacitor decreases allowing voltage signal to pass through the capacitor[15].

The capacitor has the cutoff frequency given as,

$$f_c = \frac{1}{2\pi RC} \tag{3.9}$$

The output voltage is given as,

$$V_{out} = V_{in}\left(\frac{Z_r}{Z_r + Z_c}\right) \tag{3.10}$$

The output voltage depends on the impedance of the capacitor, which eventually depends on the frequency of the signal.

Changing output voltage with respect to frequency is the major disadvantage of the simple RC filter. The order of the low pass filter is n=1. For simple applications it's reasonable but for the advanced applications, we cannot increase the order of the low pass filter. The alternative to the above circuit is op-amp based low pass filter. The bode plot of the circuit is given in Figure 3.5

Op-amp-based integrator can also be used as a low pass filter. Integrator can act as low pass filter, integrator, and inverting amplifier at various frequencies. At low frequencies, the op-amp-based integrator is used as the low pass filter, at the middle as an integrator and at high frequencies, it could be used as the inverting amplifier. The reason for such a
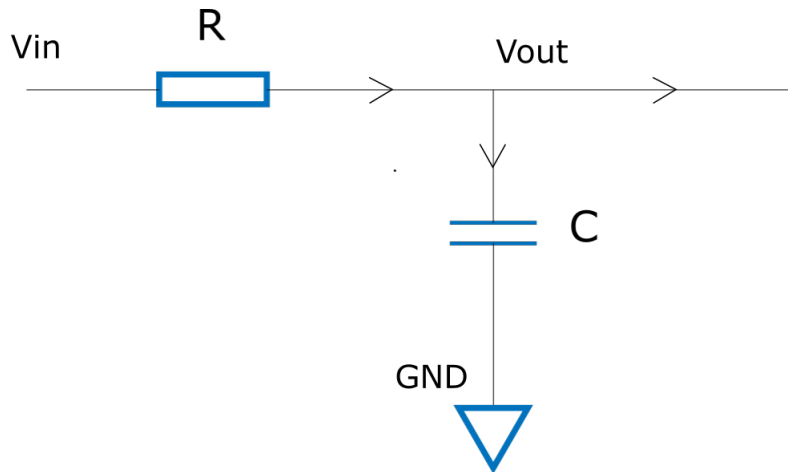
Figure 3.4: Simple RC filter. The output of the low pass filter depends on the frequency. The output not only depends upon the frequency but also on the load's frequency response.
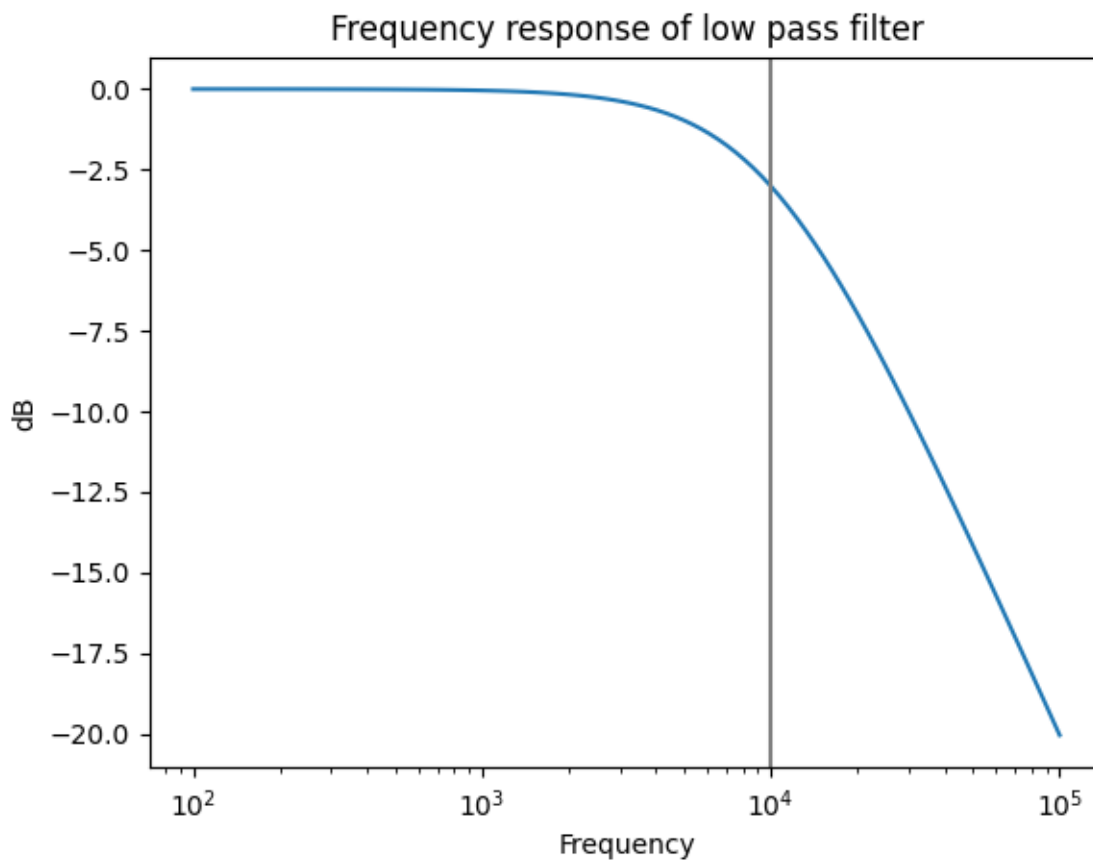

Figure 3.5: Bode Plot. Frequency response of simple low pass filter. After cutoff frequency the output decreases.
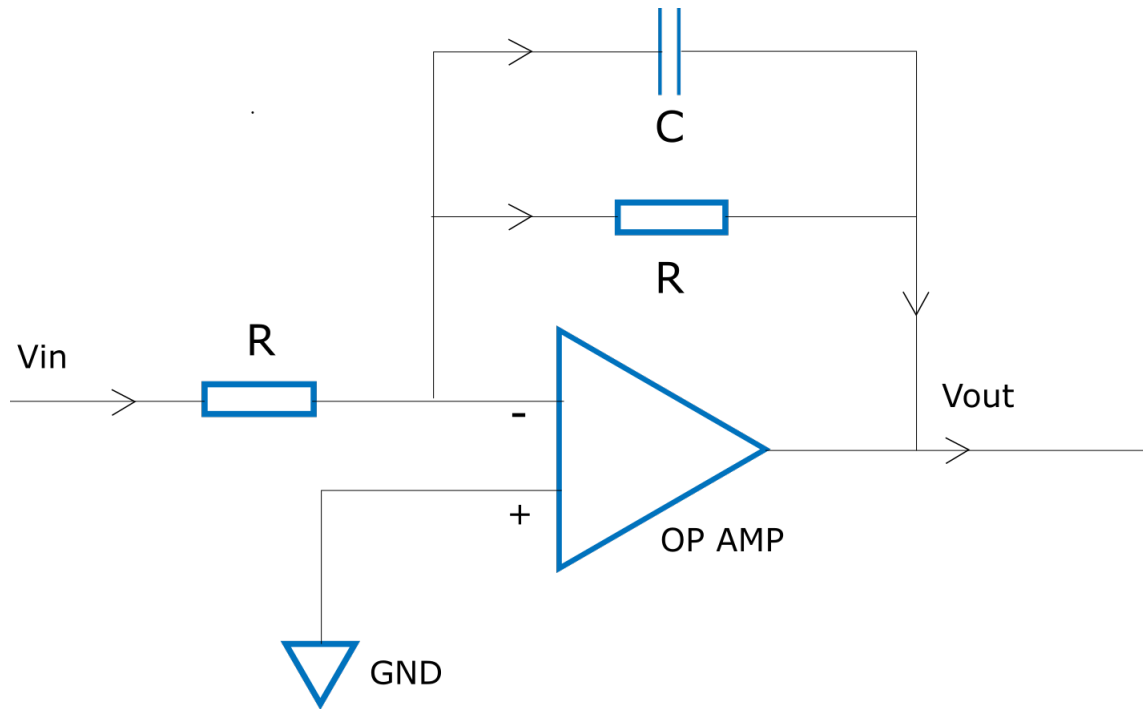
Figure 3.6: Op amp based Integrator. Op amp based integrator can be used as a low pass filter at lower frequencies.

wide variety of applications is caused by the change of impedance of the capacitor at various frequencies.

The use of the op-amp-based active low pass filter lowers the bandwidth by a significant amount. The op-amp-based integrator also solves the problem of input impedance and output impedance which cannot be solved into the simple RC-based filter. The one mentioned in the Figure 3.6 is inverting a low pass filter. The non-inverting low pass filter also has the same advantages and disadvantages except in the noninverting output voltage is inverse of the input voltage signal.

The capacitor present at the non-inverting input of the op-amp takes some finite time to charge. The time to charge up the capacitor depends upon the resistor and capacitor value. Higher the RC constant lower the cutoff frequency. This limits the PID bandwidth.
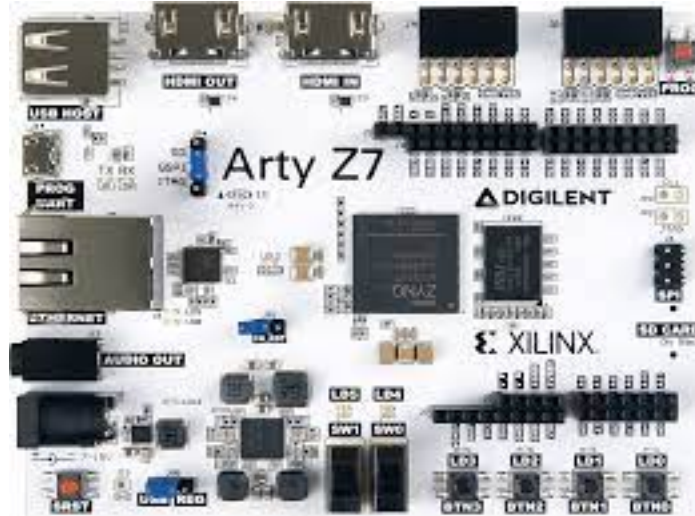
Figure 3.7: Arty z-7 20. The Arty is an evaluation board of Digilent. The Board comes with processor and hardware(FPGA).

3.4.2 FPGA based digital integrator

Integration of periodic signal can also provide information of phase. The op-amp-based integrator can be used to calculate the phase of the signal but the op-amp-based integrator is generated an "indefinite" form of integral. We need a digital-based integrator that will add all the values of the voltage in a particular amount of time. There are many candidates for digital circuits such as Arduino, Raspberry pi, and FPGA. Arduino is the simplest digital device that can be used for the digital integrator but the clock used for Arduino and analog input works on pulse width modulation(PWM). This limits the effective sensitivity and the sampling rate of the ADC. The raspberry pi is another digital circuit candidate for the digital integrator but the external ADC is needed for the pi model. This significantly reduces the bandwidth. The last candidate for the digital integrator is the FPGA. The Arty z-7 20 FPGA (Figure 3.7) has an in-built 1 MSPS ADC [16]also clock speed for the FPGA is around 120 MHz. The clock speed can also be increased to 800 MHz. This specification makes FPGA a suitable candidate for the digital integrator.
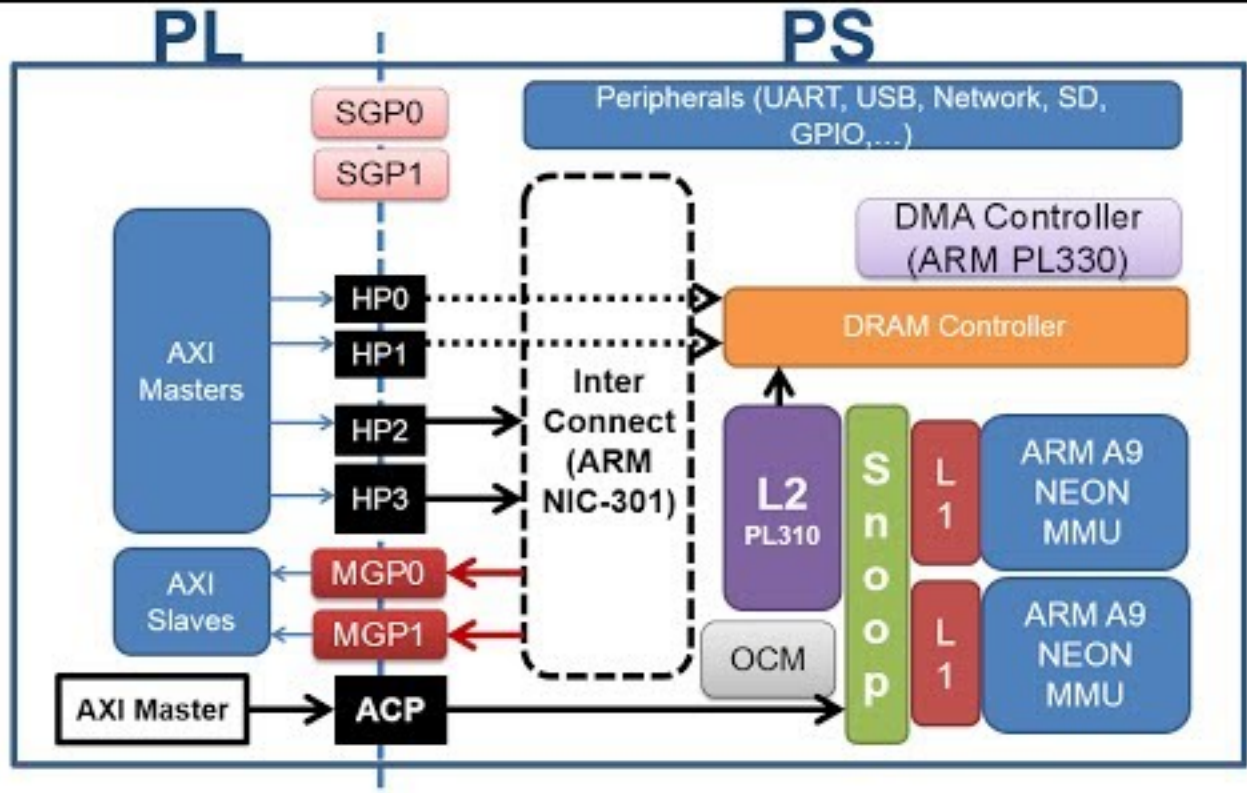
Figure 3.8: Zynq. The FPGA or PL is connected to processor(PS) with special buses such as HP's and GP's. The PS is connected external peripherals such as UART, USB.

3.5 FPGA

A field-programmable gate array (FPGA) is a device that gives access to programmable logic control over the gates. The programming language that is used for the configuration of gates is called hardware description language(HDL). There are three different types of language used in the industry around the world, Verilog, VHDL, and system-Verilog. The FPGA has evolved in the past three decades from a simple PL circuit to an advanced integrated PL-PS circuit. The use of the FPGA requires Vivado, a software built by Xilinx.

3.6 FPGA based Analog to digital converter

Vivado has default IP which does the analog to digital conversion names as XADC. The XADC module has both differential as well as absolute inputs. Here we will proceed with differential inputs. The specifications on adc are given below [17].

- **Resolution of ADC** 12 bit

- **Sampling rate of ADC** 1 MSPS

The use of the ADC in FPGA requires vivado's software development kit commonly called the SDK. The SDK uses C as a programming language to program the ADC. The control of ADC is given by assigning register values to control registers. Here different kind of registers along with their mapping has been given below.

- **CBASEADDR + 0x204** The register stores the Vp/Vn voltage value. By reading this register we get the ADC output value.

- **CBASEADDR + 0x300** The configuration register 0

- **CBASEADDR + 0x304** The configuration register 1

- **CBASEADDR + 0x308** The configuration register 2

There are plenty of registers used in the XADC module. The prominent ones are listed on the top. Control registers not only control the XADC module but working also. We can assign respective bits to XADC registers to define the mode of working. The use of such a register is not the only method to operate XADC IP. The xadc.h library is also used for the configuration of XADC IP. The use of the xadcps.h library simplifies the working of the XADC module. XAdcPsCfgInitialize, XAdcPsGetAdcData are one of the useful functions. The block diagram of the Vivado XADC is mentioned in Fig. 15.
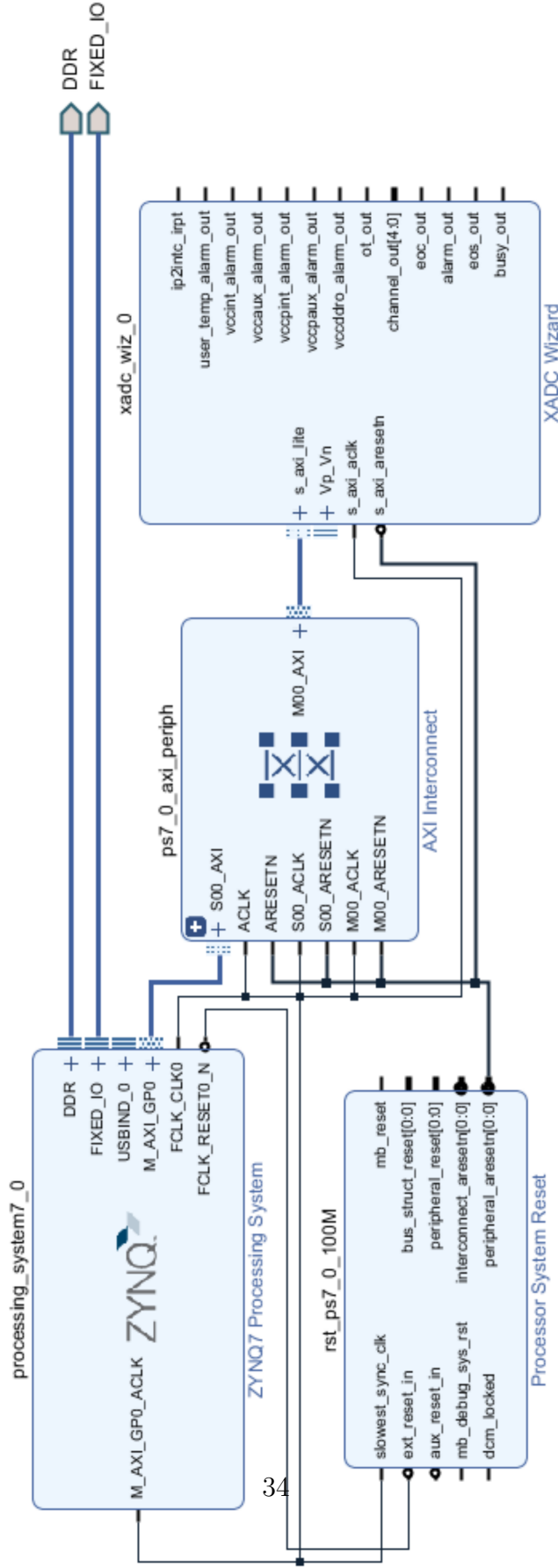
Fig. 15 Vivado block diagram for XADC wizard

The analog phase detector gives an output of 30 kHz. ADC's sampling rate is 30 kHz. If we are able to integrate the signal for a period of 33 μs We will get the phase information.
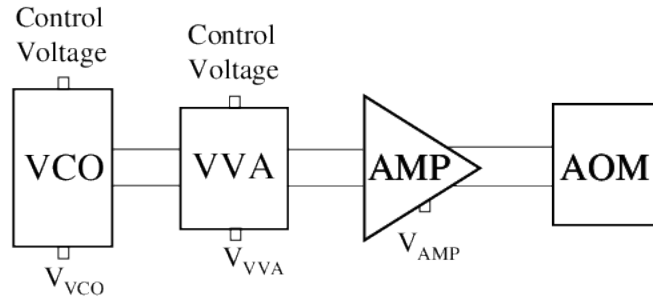
Figure 3.9: AOM Driver circuit Diagram

3.7 AOM controller

Acousto-Optic-Modulator(AOM) is the device that shifts the frequency of the laser beam with MHz offset. AOM works on the principle of diffraction generated by the mechanical strain. AOM needs an amplifier and electrical frequency signal equal to offset that needs to add or subtract from the laser beam. The following components have been used along with their application has been mentioned [18].

- **Voltage Control Oscillator** Generates the frequency of MHz range and frequency can be tuned by the voltage.

- **Variable Voltage Attenuator** Output of the VCO can be attenuated by the voltage.

- **Amplifier** Amplifies the signal of the oscillator.

The use of the AOM controller by components such as VCO, VVA adds noise to the signal. This is caused by the imperfections of the soldering. The alternative to VCO based controller is DDS. The DDS is direct digital synthesis, a digital to a radio-frequency generator that works with SPI communication. The programming of the DDS is done by a micro-controller-based evaluation board. Arduino Mega is a better candidate as it has enough pin-sets to have control over DDS. So we proceeded with other methods such as DDS.

3.8   Experimental Data

The digital FPGA based integrator is used for extraction of phase from the AD630 output signal. The output waveform is integrated for 1ms.

The XADC inbuilt analog to digital converter operating at 500 KSPS was used for the measurement. The sampling rate of the XADC cab be changed according to the needs. Sampling rate of the XADC can be made event based or the continuous mode.

Continuous mode operation works at the rate of 1 MSPS. More the sampling rate better is the summation of the incoming signal. Maximum sampling rate can be achieved by the continuous mode.

Sampling rate of 1MSPS rate is not maintained throughout operation. The need of constant XADC sampling rate is necessary for the smooth integration operation. This was the reason for the event based XADC operation.

The continuous mode operation can be converted into the event based operation. The sampling mode is changed from the software side from the PS. The usleep function can be used to change the sampling rate.

Event based XADC wizard works on the principle of the external or internal event. Current XADC IP used for the ADC works on the continuous mode.

Degree	Sum
0	783.615
10	786.441
20	792.254
30	800.701
40	802.344
50	804.143
60	805.872
70	807.47
80	809.036
90	810.925
100	812.88
110	814.163
120	813.55
130	811.904
140	810.427
150	808.779
160	807.323
170	805.74
180	804.144
190	802.659
200	800.968
210	792.883
220	788.215
230	785.543
240	783.729
250	783.188
260	782.835
270	782.828
280	782.831
290	782.822
300	782.698
310	782.535

Degree	Sum
320	782.31
330	782.01
340	782.029
350	782.561
360	783.906

Table 3.1: Phase vs Digital Integrator

The plot of the above data is plotted along with error bars in figure 3.10. The output of the ADC630 deviated from the ideal output by a large amount. Though output was derogated we were able to distinguish the different outputs for different phase differences. To lock the PID for a particular phase we need a linear region. There are two linear regions we can clearly notice and if we are able to lock out PID to the middle of the linear region, then at the start of each experiment we will have the fix phase for the optical gratings. Along with the deviated performance of the AD630, there is one major problem. The statistical error is much more than expected. This will cause a problem in locking of PI. The next task is the reduction of the statistical noise. The multi-meter can be used for the measurement of the DC voltage and graph is shown in figure 3.11 We can clearly see the working of amplitude modulation.
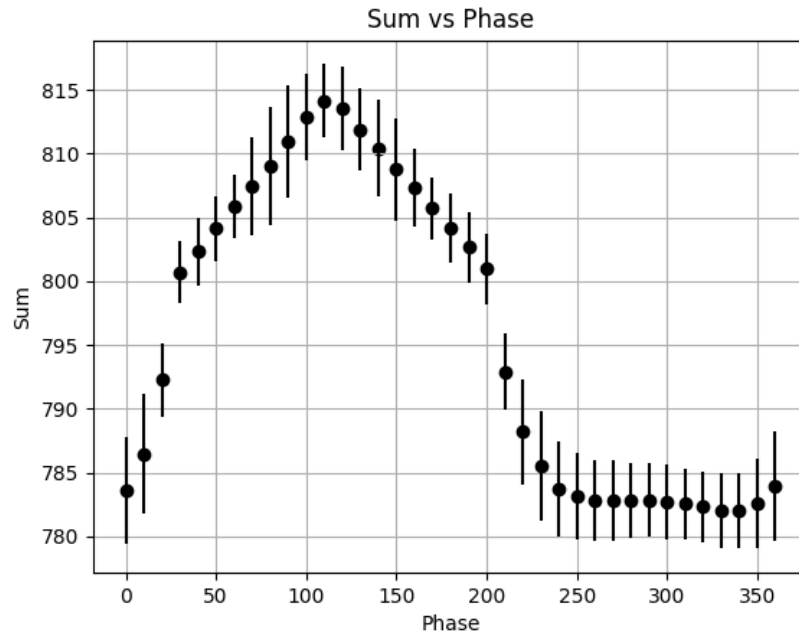
Figure 3.10: Digital Integrator data of FPGA. The characteristic of digital integrator can be seen in the graph. There
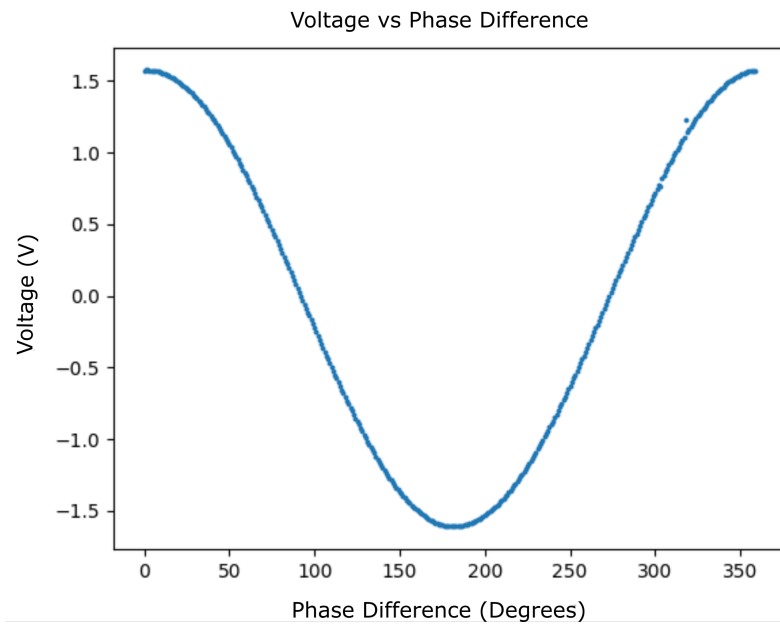are two linear regions with finite slope where we can lock the PI.

Figure 3.11: Voltage Vs Phase. The multimeter cannot be used to lock the PI but can give the DC level of an output signal of AD630.

Chapter 4

Discussion and Results

4.1 Experimental Data

As primary goal of the experiment is to measure the local acceleration due to gravity without additional phase noise. We need to make the measurement of the acceleration due to gravity by atom inteferometry. To find the local acceleration due to gravity we use following formula given as the,

$$\Phi = n \left(2\vec{k}.\vec{g}T^2 - 2\pi\alpha T^2 \right) \tag{4.1}$$

We need to find out the chirping frequency at which the total phase Φ becomes zero. There are many minimas for the equation, we need to take at least three interferometry data-sets with different interferrogram time. The Figure 4.1 shows the AI with interfereometry with 1.1 ms interferogram time. Similarly the Figure 4.2 and Figure 4.3 shows the interferometry time for the 2.27 ms and 3.3 ms respectively. When we combine all three AI graphs we get one common minima where all three graphs coincide. The Figure 4.4 shows the combination of all three graphs. We get a common minima where we can find out the local acceleration due to gravity.

When we combine all the interferometric plots we get the common minima corresponds to the actual local acceleration due to gravity. As these graphs x-axis is given in terms of chirping frequency, the local acceleration due to gravity is calculated by the
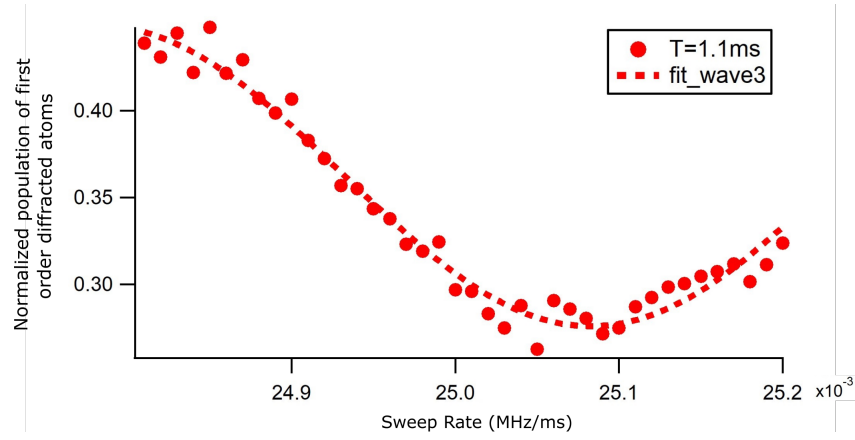
$$\alpha = \frac{\vec{k}.\vec{g}}{\pi} \tag{4.2}$$
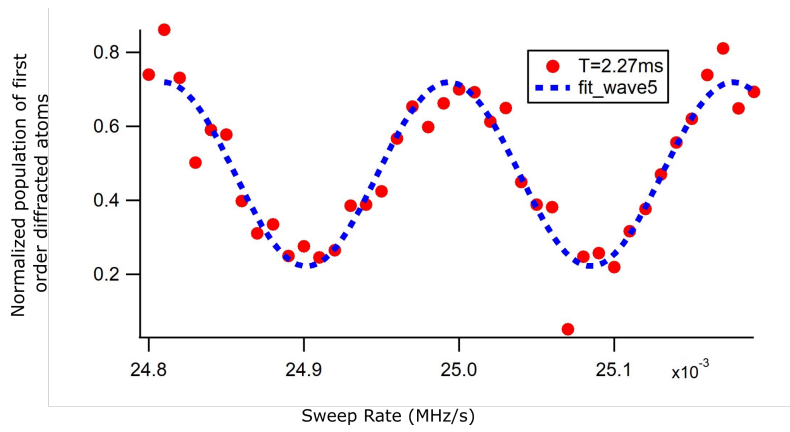
Figure 4.1: Atom interferometry with T = 1.1 ms
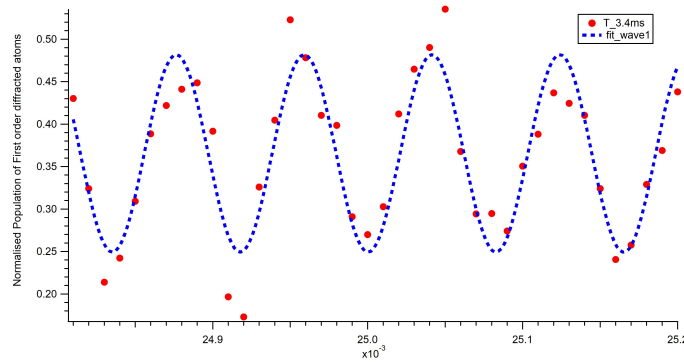

Figure 4.2: Atom interferometry with T = 2.27 ms
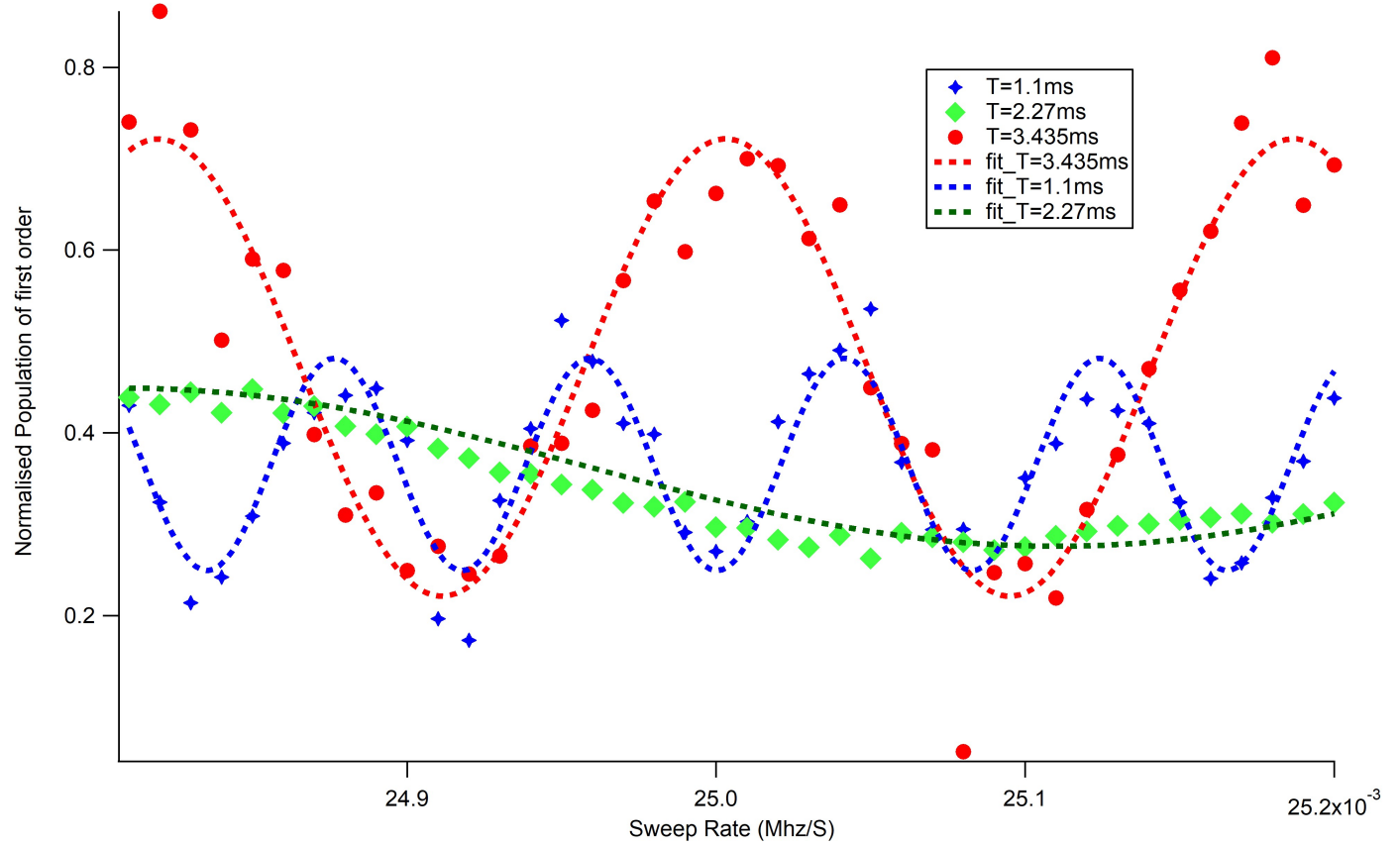

Figure 4.3: Atom interferometry with T = 3.3 ms

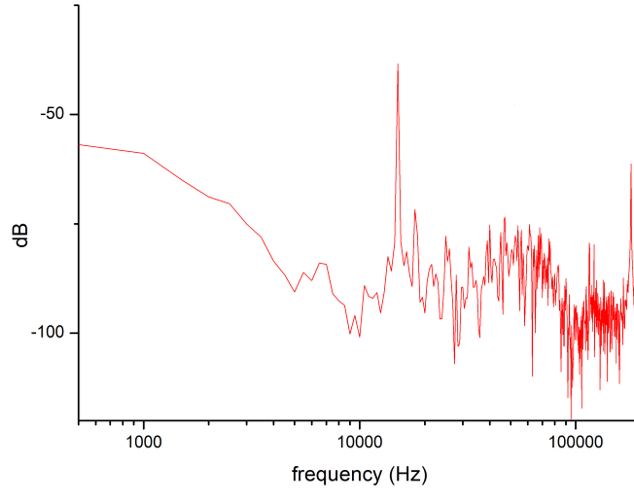Figure 4.4: All three graphs combine at one point which corresponds to the local acceleration due to gravity

Figure 4.5: Phase noise of Bragg beams

4.2 Phase Noise

The phase noise caused by the acoustic noise and vibrations is imparted in the phase of the laser beam. This can be shown here in Figure 4.5. The measurement of the phase noise is done with Fast Fourier Transform(fft). The fft clearly shows the phase noise at lower frequencies. We can also see the peak of the 15kHz signal, a standard beat frequency for Rb atom.

4.3 Results

T(ms)	$\alpha \times 10^{-3}$	g
1.1	0.0251098	9.796
2.27	0.0250942	9.790
3.435	0.0250824	9.785

Table 4.1: Interferogram Time, chirping frequency and the acceleration due to gravity for the atomic inteferometer.

The value of common local minima and their respective acceleration due to gravity is mentioned in Table 4.1. The value of local acceleration due to gravity is calculated to be 9.790 m/s^2. The phase noise cause by the vibrations has a measure impact on the precision of the calculated value. Not having a proper alignment of optical lattice beams with respect

to gravity can cause the deviation of acceleration due to gravity from actual value. The OPLL is needed for the improvement of gravimeter and future scheme is mentioned in next section.

4.4 Future Work

Most of the electrical and optical circuit has been made. The next major task is to reduce the noise in ADC of FPGA. FPGA ADC noise is much more for PI to work.

The FPGA will act as a digital PID and the analog output will be generated by the DAC. The AD1112A will be used as DAC. Output of DAC will be current so a circuit similar to the trans-impedance amplifier needs to be used which will convert the current to the voltage.

Digital integrators can be made up by two approaches. The XADC vivado IP has s-axis stream port, s-axis stream port can be fed to the custom-made IP. The custom IP's output can directly be connected to an external DAC. This method can also be used for the digital PI and will not require PS. Another approach is to connect the XADC IP to the ZYNQ processing unit. The processing unit's output can be fetched by XGPIO. XGPIO connects the internal variable to the external port. As long as the bandwidth of PI is small this approach can be used. Usually, the software is slower than the hardware.

Bibliography

[1] A mobile high-precision gravimeter based on atom interferometry.

[2] P. Bouyer, T. L. Gustavson, K. G. Haritos, and M. A. Kasevich. Microwave signal generation with optical injection locking. *Opt. Lett.*, 21(18):1502–1504, Sep 1996.

[3] S. Shahriar, Alexey Turukhin, T. Liptay, Y. Tan, and P. Hemmer. Demonstration of injection locking a diode laser using a filtered electro-optic modulator sideband. *Optics Communications - OPT COMMUN*, 184:457–462, 10 2000.

[4] M. Kasevich. Measurement of the gravitational acceleration of an atom with a light-pulse atom interferometer. *Applied Physics B*, 54:871–875, Feb 1999.

[5] Peter J. Martin, Bruce G. Oldaker, Andrew H. Miklich, and David E. Pritchard. Bragg scattering of atoms from a standing light wave. *Phys. Rev. Lett.*, 60:515–518, Feb 1988.

[6] C Tozzo and F Dalfovo. Bogoliubov spectrum and bragg spectroscopy of elongated bose-einstein condensates. *New Journal of Physics*, 5:54–54, May 2003.

[7] M. Kozuma, L. Deng, E. W. Hagley, J. Wen, R. Lutwak, K. Helmerson, S. L. Rolston, and W. D. Phillips. Coherent splitting of bose-einstein condensed atoms with optically induced bragg diffraction. *Phys. Rev. Lett.*, 82:871–875, Feb 1999.

[8] J. E. Debs, P. A. Altin, T. H. Barter, D. Döring, G. R. Dennis, G. McDonald, R. P. Anderson, J. D. Close, and N. P. Robins. Cold-atom gravimetry with a bose-einstein condensate. *Phys. Rev. A*, 84:033610, Sep 2011.

[9] M. Fox. *Quantum Optics: An Introduction*. Oxford Master Series in Physics. OUP Oxford, 2006.

[10] BOSE-EINSTEIN CONDENSATES, ATOM LASERS, Subhadeep Gupta, Aaron LEANHARDT, Alexander Cronin, and David Pritchard. Coherent manipulation of atoms with standing light waves. *Comptes Rendus de l'Académie des Sciences - Series IV - Physics*, 2, 04 2001.

[11] Peter J. Martin, Bruce G. Oldaker, Andrew H. Miklich, and David E. Pritchard. Bragg scattering of atoms from a standing light wave. *Phys. Rev. Lett.*, 60:515–518, Feb 1988.

[12] Yuan Cheng, Ke Zhang, Le-Le Chen, Wen-Jie Xu, Qin Luo, Min-Kang Zhou, and Zhong-Kun Hu. Low-phase noise and high-power laser for bragg atom interferometer. *AIP Advances*, 7(9):095211, 2017.

[13] Tunable diode lasers.

[14] https://www.analog.com/media/en/technical-documentation/data-sheets/ad630.pdf. *Analog Devices*.

[15] P. Horowitz and W. Hill. *The Art of Electronics*. Cambridge University Press, 2015.

[16] Arty z7-20: Soc zynq®-7000 development board for makers and hobbyists.

[17] 7 series fpgas and zynq-7000 soc xadc dual 12-bit 1 msps analog-to-digital converter.

[18] Daniel Mccarron. A guide to acousto-optic modulators. 03 2022.